

## Numerical Studies of Wave Generation Using Spiral Detonating Cord

K. Mahmadi<sup>1</sup>, S. Itoh<sup>2</sup>, T. Hamada<sup>2</sup>, N. Aquelet<sup>1</sup>, M. Souli<sup>1</sup>

<sup>1</sup>Université de Lille, Laboratoire de Mécanique de Lille, UMR CNRS 8107, Bd Paul Langevin, 59655 Villeneuve d'Ascq, France

<sup>2</sup>Department of Mechanical Engineering and Materials Science, 2-39-1 Kurokami, Kumamoto City, Kumamoto 860-8555, Japan

**Keywords:** Shock waves, multi-material Eulerian formulation, detonating cord, underwater explosion

**Abstract.** The control of underwater explosions is an industrial concern. In this paper, a comparison of experimental and numerical results of high-pressure generation using underwater explosion of spiral detonating cord is presented. To demonstrate that the converging process of underwater shock wave yields high pressure near the spiral center, the experimental investigation aims to compare underwater shock wave pressures obtained with several detonating cord geometrical configurations and study the wave converging process for a spiral cord. Because the experimental approach of these fast transient events is expensive and time-consuming, numerical simulations of experimental cases by using multi-material Eulerian formulation are carried out. The multi-material Eulerian, which is a particular multi-material ALE (Arbitrary Lagrangian Eulerian) formulation was successfully used in many industrial applications involving computational fluid dynamic problems. By using an explicit finite element method, a good agreement between numerical and experimental results will valid multi-material Eulerian formulation abilities to solve accurately underwater shock wave problems for spiral detonating cord in various shapes.

### Introduction

In recent years, the various processing ways using shock waves from explosions in water results in new industrial developments as non-thermal food sterilization [1], punching technique [2], and others. It is necessary to make a control of underwater shock wave to meet the industrial demands. The controls include the convergence of underwater shock waves by an appropriate technique and the adjustment of the pressure distribution of shock wave in the application.

This study mainly focuses on the numerical investigations on the underwater explosion of detonating cord in a spiral shape to obtain the converging underwater shock wave in comparison with the experimental results [3,4]. Detonating cord is a high velocity non-electric blasting accessory, flexible, easy to use and extremely safe. Detonating cord has a core of pentaerythritoltetranitrate (PETN) covered with various layers of cotton yarns and synthetic fibers. PETN is one of the strongest known high explosives. The explosion of the spiral detonating cord will be expected to result in the convergence of shock available at the nearby of the spiral center, which generates the high shock pressure.

In recent years, the necessity for numerical analysis has been increasing. The numerical investigation described in this paper aims to model this physical phenomenon by using a multi-material Eulerian scheme. This formulation has already been used with success in the simulation of fluid with large motion such as the impact and penetration problems [5]. The main advantage of the Eulerian method is that the time steps can remain roughly constant during simulations in contrast to the Lagrangian formulation where the mesh undergoes large deformations in explosions problems. Because a hydrodynamic material model requires an equation of state to define the pressure-volume relationship, we use the Jones-Wilkins-Lee-Baker equation of state for detonating cord while the Mie-Grüneisen equation of state is used for water model. The comparison between numerical and experimental results will demonstrate the capability of the multi-material Eulerian method to treat underwater explosions for detonating cord in several forms.

### Multi-material Eulerian formulation

The multi-material Eulerian method means that the material flows through a fixed mesh and two or more different materials can be mixed within the same fixed mesh.

**Lagrangian phase.** A Lagrangian phase is performed, in which the mesh moves with the material, in this phase the changes in velocity an internal energy due to the internal and external forces are calculated. The equilibrium equations are:

$$\frac{\partial \rho}{\partial t} = -\rho \frac{\partial v_i}{\partial x_i}, \quad \rho \frac{\partial v_i}{\partial t} = \sigma_{ij,j} + \rho b_i, \quad \rho \frac{\partial e}{\partial t} = \sigma_{ij} v_{i,j} + \rho b_i v_i \tag{1}$$

where  $v_i$  is the velocity of the material,  $\sigma_{ij}$  is the Cauchy stress and  $e$  is the internal energy.

After the Lagrangian phase is performed, either the stress tensor, pressure and deviatoric stress should be equilibrated, but most mixture theories equilibrate only pressure, the pressure equilibrium is a non-linear problem, which is complex and expensive to solve. Skipping the stress equilibrium phase is assuming an equal strain rate for both materials, which is incorrect. For most problems, the linear distribution based on volume fraction of the volumetric strain during the Lagrangian phase also leads to incorrect results. The volume distribution should be scaled by the bulk compression of the two materials in the element. Now, to determine the volume distribution in a ALE cell, the material interface position must be known.

There are several methods to treat the material interface in a fluid problem; the common one is the MAC method, which involves Eulerian flow calculation and Lagrangian particle movement.

Another possible way of tracking interfaces is the use of the volume fractions of the elements, or the Young method [6]. The Young method is developed to track an interface in elements containing two materials for two-dimensional problems. This method is adapted in this paper for the two dimensional problems.

The interface position is used to calculate the volume of the fluid flowing across cell sides. The interface calculation prevents advection of very small fluxes between partially filled and empty elements. Instead fluid flow is transported from ‘filled’ element to ‘empty’ element and this change in volume will be monitored and used to ‘fill-up’ the element or increase its volume fraction.

**Advection phase.** In the second phase, the transport of mass, momentum and internal energy across the element boundaries is computed. This phase may be considered as a ‘re-mapping’ phase. The displaced mesh from the Lagrangian phase is remapped into the initial mesh for an Eulerian formulation, or an arbitrary distorted mesh for an ALE formulation.

In this advection phase, we solve a hyperbolic problem, or a transport problem, where the variables are density, momentum per unit volume and internal energy per unit volume. Details of the numerical method used to solve the equations are described in detail in [6] and [7], where the Donor Cell algorithm, a first order advection method and the Van Leer algorithm, a second order advection method [8] are used. As an example, the equation for mass conservation is:

$$\frac{\partial \rho}{\partial t} + \nabla \cdot (\rho u) = 0 \tag{2}$$

These algorithms have already been described in detail by some authors [7, 9].

### Jones-Wilkins-Lee-Baker (JWL) equation of state used for detonating cord

We used this equation of state for detonating cord. The JWL equation-of-state was recently developed by Baker and is further described by Orosz [10]. The derived form of the equation of state is based on the Jones-Willkins-Lee (JWL) form due to its computational robustness and asymptotic to an ideal gas at high expansions.

Table 1 JWL parameters for detonating cord

A1 (Mbar)	A2 (Mbar)	A3 (Mbar)	A4 (Mbar)	R2	R1	R3	R4
521.96	71.104	4.4774	0.97725	8.7877	44.169	25.072	2.2251

C (Mbar)	$\omega$	$A\lambda_1$	$B\lambda_1$	$R\lambda_1$	$A\lambda_2$	$B\lambda_2$	$R\lambda_2$
0.1570	0.32357	12.257	52.404	43.932	8.6351	-4.9176	2.1303

Additional experimental terms and a variable Gruneisen parameter have been added to adequately describe the high pressure region above the Chapman-Jouguet state.

The JWL thermodynamic equation of state enables the accurate representation of the P-V behaviour of explosives. This relationship, which is an extension of the commonly used Jones-Wilkins-Lee relationship, can be expressed as

$$p = \sum_{i=1}^5 A_i \left(1 - \frac{\lambda}{R_i V}\right) e^{-R_i V} + \frac{\lambda E}{V} + C \left(1 - \frac{\lambda}{\omega}\right) V^{-(\omega+1)}, \quad \lambda = \sum_{i=1}^5 A_i (A_{\lambda i} V + B_{\lambda i}) e^{-R_i V} + \omega \quad (3)$$

where  $V$  is the relative volume and  $A_i$ ,  $R_i$ ,  $A_{\lambda i}$ ,  $B_{\lambda i}$ ,  $R_{\lambda i}$ ,  $C$ , and  $\omega$  are input constants defined above. Table 1 gives the JWL parameters for detonating cord.

### Mie-Grüneisen equation of state used for water

In our study, the water was modelled with Mie-Grüneisen equation of state with the parameters as given in table 2.

The Mie-Grüneisen equation of state with cubic shock velocity-particle velocity defines pressure for compressed materials as

Table 2 Grüneisen parameters for water

$\rho_0$ (g/cm <sup>3</sup> )	$\gamma_0$	C (mm/ $\mu$ s)	S
1.00	0.1	148	1.92

$$p = \frac{\rho_0 C^2 \mu \left[1 + \left(1 - \frac{\gamma}{2}\right)\right] \mu}{1 - (S - 1)\mu} + \gamma_0 E \quad (4)$$

where  $C$  is the intercept of the particle velocity behind the shock front,  $u_p$ , versus shock velocity,  $u_s$  curve respectively;  $S$  is the coefficient of the slope of the  $u_s$ - $u_p$  curve ( $u_s = C + Su_p$ );  $\gamma_0$  is the initial Grüneisen gamma and  $\mu = (\rho/\rho_0) - 1$ . The Grüneisen gamma is defined by the Mie-Grüneisen equation of state, Equation (5) related the pressure,  $p$  to the internal energy per unit volume,  $E$ .

$$p = p_h + \gamma(E - E_h) \quad (5)$$

where the subscript  $h$  defined the Hugoniot jump values given by equations (6).

$$\rho_0 u_s = \rho(u_s - u_p), \quad p_h = \rho_0 u_s u_p, \quad E_h = p_h(V_0 - V)/2 \quad (6)$$

### The artificial viscosity method

A widely used method for correcting the discontinuities is the addition of an artificial viscosity, which spreads the shock wave over three or four mesh points and so regularized the discontinuity. Bulk viscosity is proposed in one spatial dimension by Von Neumann and Richtmyer [11]. They introduced a pressure-like term, designated  $q$  that is added consistently to the pressure,  $P$ , in all of the governing equations.

$$\rho \frac{\partial u}{\partial t} = -\frac{\partial(P + q)}{\partial x}, \quad \frac{\partial \varepsilon}{\partial t} = -(P + q) \frac{\partial u}{\partial x} \quad (7)$$

Later researchers added a linear term to eliminate the remaining oscillations behind the shock [12].

$$q = C_q \rho (\Delta u)^2 + C_L a \rho |\Delta u| \quad (8)$$

where  $q$  is the shock viscosity,  $C_q$  is the quadratic viscosity coefficient,  $\rho$  is the density,  $\Delta u$  is the velocity jump across a shock,  $a$  is the speed of sound and  $C_L$  is the linear viscosity coefficient. Typical values used in calculations for  $C_q$  and  $C_L$  are 1.5 and 0.06 respectively.

**Finite element models**

Only cases V, VI, VII and VIII when Dh=50mm are chosen for the numerical study. The explosion of a detonating cord generates an immense pressure in water. A detonation wave propagates at great constant speed (6308m/s). A chemical reaction occurs producing large quantities of gas in a short period of time. The density of detonating cord used is 1.2g/cm<sup>3</sup>.

The three-dimensional model represented in figure 1 has been discretized in the case V into 287745 8-noded brick elements and 319200 nodes. The ignition of the explosion is applied at the point O (2.3485, 0, 0). The position of pressure measurement is shown in figure 2, which sketches experimental devices.

Figure 3-5 present the model of the spiral detonating cord in water. The ignition of the explosion is applied at the point O (59, 0, 0) (Case VI), O (99, 0, 0) (Case VII), O (36.7145, 0, 0) (Case VIII).

Table 3 Experiment condition

FORM OF DETONATING CORD		LENGTH OF DETONATING CORD	Dh
(V) STRAIGHT		250mm	50mm
SPIRAL	(VI) r1=60mm	250mm	50mm
	(VII)r1=100mm	400mm	50mm
(VIII) CIRCLE		250mm	50mm

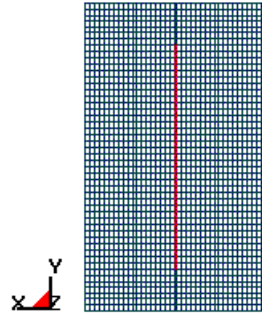


Fig.1 Model of case V, form of detonating cord: straight, Dh=50mm

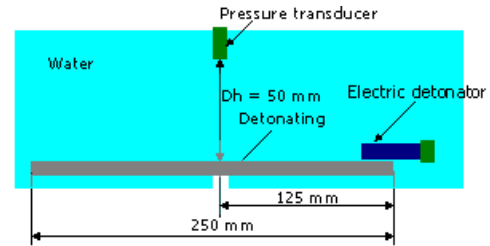


Fig.2 Case V, Form of detonating cord: Straight

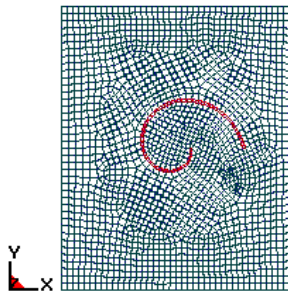


Fig.3 Model of case VI

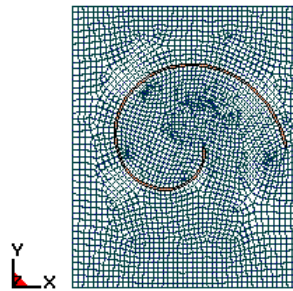


Fig.4 Model of case VII

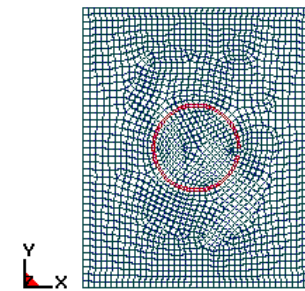


Fig.5 Model of case VIII

**NUMERICAL RESULTS**

In this section, we present numerical results for several cases of detonating cord underwater explosion. The pressure histories with multi-material Eulerian formulation are plotted in figures 7,9,11 and 13. The numerical overpressure representing the pressure jump measured at Dh=50 mm.

Figures 6(a) and (b) show the plots of pressures taken in the propagating process of the shock wave.

The plots have 5 μs inter-frame time in figure 6(a) and in figure 6(b) is 2μs. The objective of these plots is to indicate the convergence of underwater shock wave of the detonating cord. Both figure 6

(a) and figure 6(b) allow to show clearly the convergence of underwater shock wave when using spiral detonating cord.

**Case V.** The pressure history at Dh=50mm, for which the Eulerian results were captured, is as shown in figure 7. Experimental curve is presented in the same figure. The experimental overpressure is 176.5MPa while the numerical peak value is 175.88MPa. Figure 8 gives the propagation of pressure for case V at t=12μs, 24μs and 36μs.

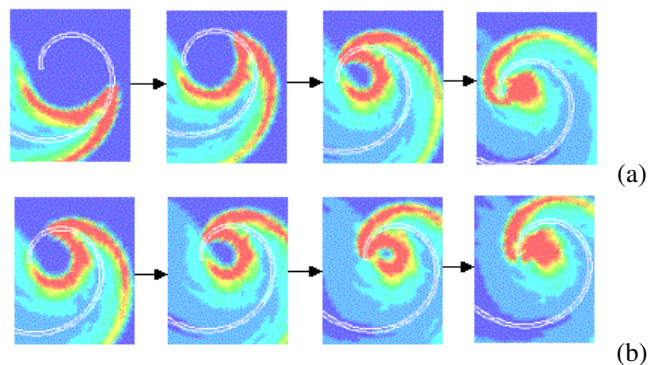


Fig.6 Numerical plots of pressures

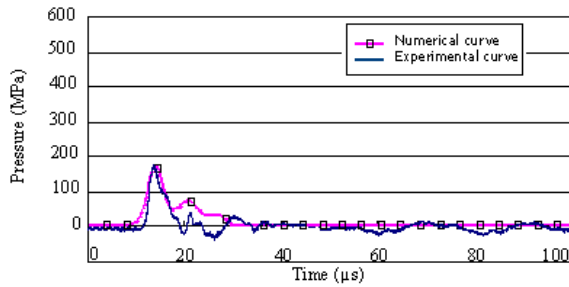


Fig.7 Case V: Numerical and experimental curves of pressure-time at  $D_h=50\text{mm}$

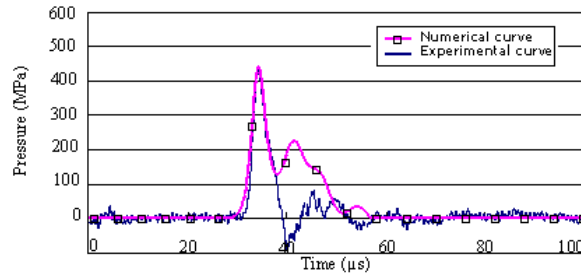


Fig.9 Case VI: Numerical and experimental curves of pressure-time at  $D_h=50\text{mm}$

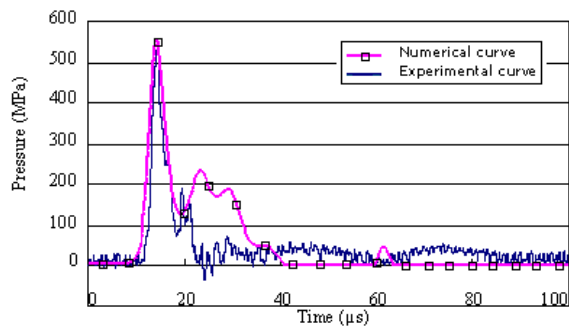


Fig.11 Case VII: Numerical and experimental curves of pressure-time at  $D_h=50\text{mm}$

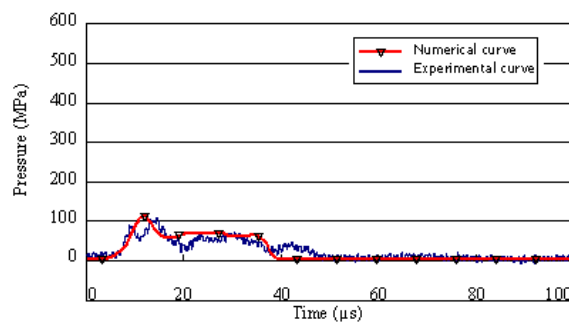


Fig.13 Case VIII: Numerical and experimental curves of pressure-time at  $D_h=50\text{mm}$

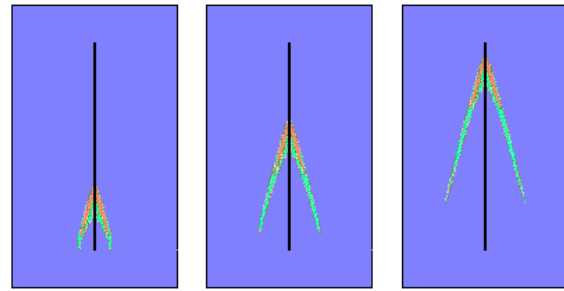


Fig.8 Pressure profile at  $t=12\mu\text{s}$ ,  $24\mu\text{s}$  and  $36\mu\text{s}$

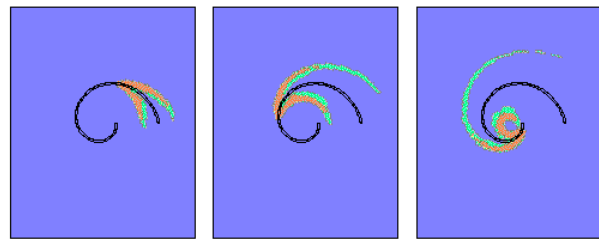


Fig.10 Pressure profile at  $t=10\mu\text{s}$ ,  $20\mu\text{s}$  and  $30\mu\text{s}$

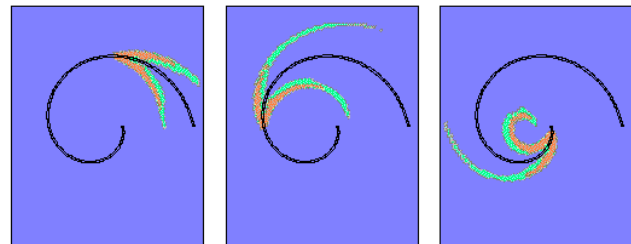


Fig.12 Pressure profile at  $t=18\mu\text{s}$ ,  $36\mu\text{s}$  and  $54\mu\text{s}$

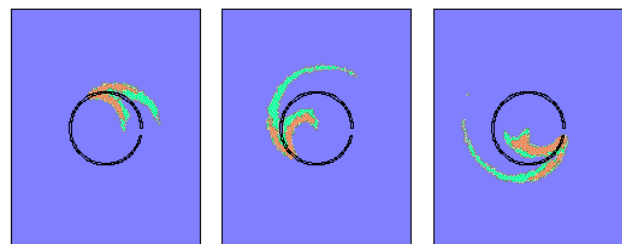


Fig.14 Pressure profile at  $t=12\mu\text{s}$ ,  $24\mu\text{s}$  and  $36\mu\text{s}$

**Case VI.** The pressure profile at  $D_h=50\text{mm}$  for which the detonating cord is spiral, is as shown in figure 9. Experimental curve is superposed in the same figure. The experimental overpressure is  $440\text{MPa}$  while the numerical overpressure is  $440.92\text{MPa}$ . Figure 10 shows the propagation of pressure for case VI at  $t=10\mu\text{s}$ ,  $20\mu\text{s}$  and  $30\mu\text{s}$ .

**Case VII.** As shown in figure 11, experimental curve is superposed with numerical pressure history. The experimental peak value is  $539.5\text{MPa}$  while the numerical overpressure is about  $550.6\text{MPa}$ . Figure 12 gives the propagation of pressure for case VII at  $t=18\mu\text{s}$ ,  $36\mu\text{s}$  and  $54\mu\text{s}$ .

**Case VIII.** Figure 13 gives the experimental curve superposed with the numerical curve. In this case, the experimental overpressure is 109.3MPa and the numerical overpressure is 106.77MPa. Figure 14 gives the propagation of pressure for case VIII at  $t=12\mu\text{s}$ ,  $24\mu\text{s}$  and  $36\mu\text{s}$ .

Table 4 Comparisons of the pressure peak in experimental and numerical cases

	Overpressure (MPa)			
	CASE V	CASE VI	CASE VII	CASE VIII
Experimental results	176.5	440	539.5	109.3
Numerical results	175.88	440.92	550.6	106.77
Relative Error (%)	0.35	0.20	2.05	2.31

Table 4 presents the summary of the experimental and simulation overpressures. In the four cases, the relative error between the experimental and numerical jump pressure values show that the multi-material Eulerian formulation gives good agreement with experimental results.

## Conclusion

This study demonstrates that the underwater shock wave from a specially designed spiral shape of detonating cord converges at the spiral center to increase the shock pressure. The impulse of shock wave also is able to be improved at distance  $D_h=272\text{mm}$ . A numerical investigation was presented in order to demonstrate the abilities of the multi-material Eulerian method to simulate the underwater explosion problems. Comparing the overpressure values at  $D_h=50\text{mm}$  for several cases reveals a maximum relative error under 2.5%. The multi-material Eulerian formulation can predict the pressure history of underwater explosion from detonating cord in various shapes.

## References

- [1] K. Fujiwara, T. Hiroe, M. Asaoka, Shock sterilization of dry powder foods, *Journal of Pressure Vessel Technology*, Trans. ASME, Vol. 460 (2003) pp 271-276.
- [2] S. Itoh, S. Nagano, M. Fujita, The features of the Assembly for Punching of Pipes by Using the Converging Underwater Shock Wave, *Proceedings of the Symposium of J. S. M. E.*, Vol.948-3, 1994.
- [3] S. Itoh, S. Nagano, T. Hamada, K. Murata and Y. Kato ; "High Pressure Generation Using the Underwater Explosion of Spiral Detonation Cord ", 2000 ASME PVP Conf., EMERGING TECHNOLOGIES IN FLUIDS, STRUCTURES, AND FLUID/STRUCTURE INTERACTIONS, July 2000, PVP-Vol. 414-2 pp. 81-85.
- [4] S. Itoh, T. Hamada, S. Nagano, K. Murata and Y. Kato ; "Underwater shock focusing using the explosion of spiral detonating cord", *The 23rd Inter. Symp. on Shock Waves*, Fort Worth, Texas, USA, July, 2001, p236
- [5] D.J. Benson, A Multi-Material Eulerian Formulation for the efficient solution of impact and penetration problems, *Computational Mechanics*, Vol.15 (1995) pp 558-571.
- [6] D.L. Young, Time-dependent multi-material flow with large fluid distortion, *Numerical Methods for Fluids Dynamics*, Ed. K. W. Morton and M.J. Baines, Academic Press, New-York (1982).
- [7] D. J. Benson, Momentum Advection on a Staggered Mesh, *Journal of Computational Physics*, Vol.100, No.1 (1992) pp.143-162.
- [8] B. Van Leer, Towards the Ultimate Conservative Difference Scheme. IV. A New Approach to Numerical Convection, *Journal of Computational Physics* Vol.23 (1977) pp 276-299.
- [9] M. Souli, A. Ouahsine and L. Lewin, ALE formulation for fluid-structure interaction problems, *Computer Methods in Applied Mech. and Eng.* Vol.190 (2000) pp659-675.
- [10] J.O. Hallquist, LS-DYNA, Theoretical Manual, Livermore Software Technol. Corp., Livermore, 1998.
- [11] J. Von Neumann, R.D. Richtmyer, A method for the numerical calculation of hydrodynamics shocks, *J. Appl. Phys.* Vol. 21 (1950).
- [12] D.J. Benson, Computational methods in Lagrangian and Eulerian hydrocodes, *Comput. Methods Appl. Mech. Engrg.* Vol.99 (1992) pp235-394.